

Received January 8, 2021, accepted January 14, 2021, date of publication February 1, 2021, date of current version February 16, 2021.

Digital Object Identifier 10.1109/ACCESS.2021.3056110

# A Novel Method of On-Line Coal-Rock Interface Characterization Using THz-TDs

JING YU<sup>1,2</sup>, XIN WANG<sup>1,3</sup>, ENJIE DING<sup>1</sup>, AND JIANGBO JING<sup>1</sup>

<sup>1</sup>IoT Perception Mine Research Center, China University of Mining and Technology, Xuzhou 221000, China

<sup>2</sup>School of Information and Electrical Engineering, China University of Mining and Technology, Xuzhou 221000, China

<sup>3</sup>Jiangsu Vocational Institute of Architectural Technology, Xuzhou 221000, China

Corresponding author: Xin Wang (wang3880816@qq.com)

This work was supported in part by the National Natural Science Foundation of China under Grant 52074273, and in part by the Open Fund of the National and Local Joint Engineering Laboratory of Mining Internet Application Technology under Grant Khkf20180102.

**ABSTRACT** The core problem in unmanned/intelligent working face of coal mining is the automatic adjustment of shearer arm where the coal-rock interface detection is the key. The cutting location of shearer drum affect the proportion of coal and rock powder around the cutting teeth of shearer drum. Therefore, the method of on-line coal rock interface characterization using Terahertz Time Domain spectroscopy (THz-TDs) we proposed aims to estimate the ratio of rock by Terahertz response. Firstly, anthracite and quartz sandstone were uniformly mixed according to 39 different ratios in this study, the samples' responses were obtained by terahertz system, and then the obtained time domain data was converted into frequency domain data by fast Fourier transform. The absorption coefficient spectrum and the refractive index profile of the 39 samples were calculated by optical parametric model. Secondly, corresponding quantitative model between mixed coal/rock powder and THz signal was built by using back propagation neural network (BPNN) and least squares support vector machine (LSSVM). We expected to use the ratio of rock powder detected by the model to estimate the depth of shearer drum teeth embedded in the rock layer. Finally, we found that both two mathematical arithmetic is feasible to quantitatively detect different proportion of coal and rock mixtures. The results show that the depth of shearer drum teeth embedded in the rock layer could be estimated by the novel method, which means the coal-rock interface could be on-line characterized by using THz-TDs and the height of the drum could be adjusted in time.

**INDEX TERMS** Terahertz, quantitative detection, least squares support vector machine, back propagation neural network.

## I. INTRODUCTION

Drum shearer is one of the most commonly equipment used in coal mining face, having widely applied to thick, medium and thin coal seam mining [1]. And the drum is the key component of shearer cutting and conveying coal [2]. At present, the adjustment of shearer arm during coal mining mainly depends on the perception of coal-rock interface by artificial experience including visual observation and observation of vibration noise emitted during cutting [3]. However, a large number of dust particles produced by the shearer during coal cutting are not only harmful to personnel health, but also has potential explosion [4]. In addition, once the drum of shearer cuts through the rock, it will accelerate the aging of the drum cutting teeth [5], [6]. The automatic/unmanned mining

technology is a high-efficiency safe mining method, which can solve the core problem of traditional mining method [7].

Identification of coal-rock interface is a key link of unmanned mining technology, relating to the accurate cutting of deep coal mining by shearer. Many researchers have proposed some methods on identification of coal and rock interface to achieve unmanned mining work face. In our previous work, we explored the physical properties of coals/rocks in THz band, and achieved fast, efficient and accurate classification of coal and rock by the means of principal component analysis, support vector machine, and THz spectral data. Finally, a stable coal-rock identification model of THz-SVM is proposed [8]. Wang *et al.* proposed a method of dynamic identification in a coal-rock interface based on the fusion of adaptive weight optimization and multi-sensor information. To research significant differences in the signals such as the cutting current, vibration, acoustic emission, and infrared thermography under diverse cutting ratios,

The associate editor coordinating the review of this manuscript and approving it for publication was Qichun Zhang<sup>1</sup>.

seven coal-rock mixture test specimens with different proportion are analyzed. Finally, both the detection accuracy and detection speed of the method has been verified [9], [10]. Zhang *et al.* proposes a diagnosis method based on bimodal deep learning and Hilbert-Huang transform, and they employs the mechanical vibration and acoustic waves of a hydraulic support tail beam for an accurate and fast coal-rock recognition. Finally, the comparison of experimental results demonstrates the superiority of the proposed method in terms of recognition accuracy [11], [12]. In [13], Si *et al.* take the sound signal, Y-axis and Z-axis vibration signals as analytic objects and proposes a fusion recognition method for shearer coal-rock cutting state based on improved radical basis function neural network and Dempster-Shafer evidence theory. Experiment show that this method can effectively identify the cutting state of coal and rock [14].

Even though the above technologies have realized the identification of coal and rock interface to some extent, there still exist many problems, such as unreliable signal-to-noise ratio, real-time data collection, and the control of drum height due to the harsh underground mining environment. Even a serious time lag problem and misjudgment problem exist in the unitary coal-rock identification system established in our original scheme, which can only detect accurately when the cut is all rock. In this study, we adopt binary or even multiple hybrid systems in the process of sampling, and proposed a method for on-line coal-rock interface characterization using Terahertz Time Domain spectroscopy (THz-TDs). Terahertz wave is electromagnetic radiation between microwave and infrared band. Its frequency band is usually between 0.1~10THz. The advantages of terahertz radiation include high coherence, low energy, selective transmittance, safety and so on [15]–[17]. Our application scenario is coal mine, where there is a great difference in chemical composition between coal and rock, and literature [11] proves that this difference is very significant in terahertz frequency band. This indicates that THz-TDs is very promising for coal-rock interface characterization compared with other methods.

The depth of the drum embedded in the rock determines the ratio of rock powder around the drum to the surrounding dust, which provides a meaningful basic for characterizing the coal-rock interface. In order to realize the detection of respective proportion of coal and rock, we analyzed the relationship between rock ratio and the THz signal by principal component analysis (PCA) before that. Two kinds of THz signals, absorption coefficient and refractive index within 0.4THz~2THz frequencies, were extracted as modeling objects. Simultaneously, due to compare the robustness of the model, BPNN and LSSVM were used to build different detection models respectively.

Quantitative model of coal and rock is one of the most important research contents in this article. Moreover, considering that the dust around the drum is floating in the air during actual mining process. The samples collected in the mine are actually dust and air, both of which are in a state of gas-solid two-phase flow. Since dynamic samples are difficult

to extract, high density polyethylene (HDPE) was used to replace air in the sample preparation process for simulating the static state of gas-solid two-phase flow. HDPE is a non-polar thermoplastic resin with high crystallinity. HDPE is chosen to replace the air in the sample mainly because it has almost zero absorption to the terahertz light wave, and the other HDPE has the function of sticking when mixed with the coal/rock [18]. In this article, polyethylene was added to the sample to change the sparsity of the sample, and the most sensitive sparsity range to terahertz wave was studied.

Finally, we established a theoretical model based on the relationship between rock ratio and the depth of rock layer cut by drum. Once the rock ratio is detected, the model can estimate the depth of the cut in time, which provides a theoretical basis for future unmanned mining and further research.

## II. EXPERIMENTED METHODS

### A. EXPERIMENTED DEVICE

The harsh mining environment and high humidity in underground coal mines require a complete coal-rock interface characterization system for sampling and detecting coal-rock samples. Fig.1 is the Schematic diagram of on-line coal-rock interface characterization system.

As shown in the Fig.1, when entering the sampling device, the coal and rock powder first passes through the particle size control area. According to the available literature [19], the regression particle size of powder with particle size below  $74\mu\text{m}$  is closer to the target value. Therefore, all samples used in the subsequent experiments are standard samples, and the particle size is controlled below  $74\mu\text{m}$ . Part 2 in Fig.1 is drying area. In order to achieve the best detection effect, the samples need to be in a dry state or under uniform humidity to exclude the influence of humidity on THz. The part 3 is the sparsity control area. Terahertz wave is significantly sensitive to sparsity degrees of sample. It is very necessary to maintain the high sensitivity and uniformity of sample sparsity. The sparsity can be controlled by properly controlling the flow velocity of the sample. The collected powder passes through the part 3, representing the successful sampling. Part 4 is the THz detection system. Samples enters the part 4 in a state of gas-solid two-phase flow, and the mass ratio of rock is predicted by the coal-rock quantitative detection model. Part 5 is the coal-rock interface characterization system, which estimates the height of the rock strata cut by the shearer through the rock ratio and timely adjusts the height of the shearer arm, and finally realize the automatic control of the shearer arm in the underground coal mining face.

In the experimental process of terahertz signal extraction, the equipment we used is the TAS7500SP transmission type of terahertz time domain spectrometer made by Advantest Company of Japan, and the resolution of the system is 7.6 GHz. Its working frequency range from 0.1THz to 4THz, the scanning speed is less than 8ms/scan, and the peak dynamic range is more than 70 DB. The terahertz spectral system uses femtosecond optical pulse to generate and detect

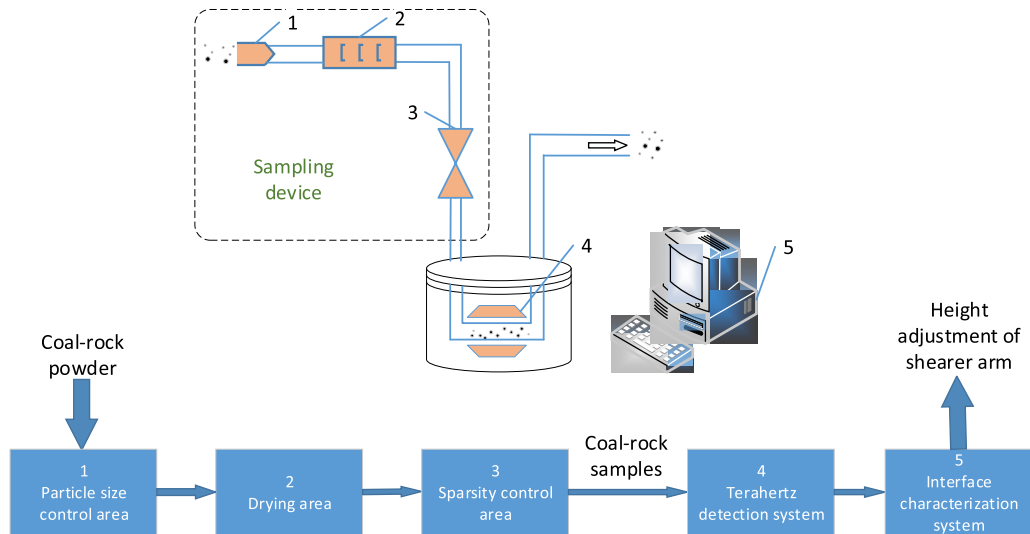


FIGURE 1. Schematic diagram of coal-rock interface characterization system.

TABLE 1. Standard value and uncertainty of standard material for physical properties and chemical composition gap of national coal.

Total sulfur (%)	Ash content (%)	Volatile matter (%)	Calorific value (%)	Carbon (C) (%)	Hydroge n (H) (%)	Nitrogen (N) (%)	Relative density in a vacuum (20°C)
2.19	25.10	28.55	24.65	60.18	3.89	1.02	1.54
0.09	0.17	0.36	0.15	0.49	0.19	0.07	0.03

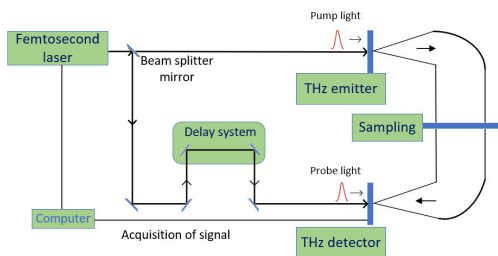


FIGURE 2. Schematic diagram of transmission THz-TDs system.

terahertz pulse, which works as shown in Fig. 2. The pulse emitted by femtosecond laser is divided into two parts of the light beam when it enters the system, in which the pump light illuminates the transmitter and generates a terahertz pulse. Then the terahertz pulse travels for a distance in free space and focuses on the detector. The transient generated by terahertz induction in the detector can be measured by detecting pulse. Terahertz pulse is generated by transient current of photoconductive antenna or optical rectifier of nonlinear optical crystal. Since THz-TDs can cause the amplitude and phase of the terahertz radiation, the absorption and dispersion effect generated when the THz pulse passes through the sample can be obtained by analyzing the signal in the frequency domain [20]–[25]. In order to avoid the absorption of the

water vapor in the air to the terahertz wave and improve the signal-to-noise ratio of the spectrum, the sealed sample area is filled with nitrogen, the indoor is put into a dehumidifier, and the whole experiment is carried out in a closed laboratory at room temperature of about 26 degrees.

**B. SAMPLE PREPARATION**

In this article, we prepared tablet samples with different mass ratio to study the differences of coal-rock mixed tablets with different mass ratio, and to establish a quantitative detection model of coal-rock, thus achieving part 4 of Fig. 1. A quantitative detection model is established for estimating the height of the drum embedded strata through the rock ratio, and to realize the coal-rock interface characterization and timely adjust the height of the shearer. In this experiment, we prepared 39 coal-rock mixture samples with different mass ratios. The coal and rock are unified. The coal powder is a standard sample of bituminous coal, and the rock powder is a standard sample of the quartz sandstone extracted from Tong ling, Anhui. The main standard value and the uncertainty of the chemical components of the two standard matter are shown in Table 1, Table 2.

Before preparing the samples, the coal powder and the rock powder was ground by an agate mortar for reducing the influence of the spectral scattering and screened out through

**TABLE 2. Identification value and uncertainty of standard materials for rock composition analysis.**

	Pr	Rb	S	Sb	Sc	Se	Sm	Sn
Mass	5.4	29	860	0.6	4.2	0.08	4.7	1.1
fraction (10 <sup>-6</sup> )	± 0.6	± 2	± 42	± 0.11	± 0.3	± 0.03	± 0.3	± 0.2
	S <sub>i</sub> O <sub>2</sub>	Al <sub>2</sub> O <sub>3</sub>	TFe <sub>2</sub> O <sub>3</sub>	FeO	MgO	CaO	Na <sub>2</sub> O	K <sub>2</sub> O
Mass	90.36	3.52	3.22	0.61	0.082	0.3	0.061	0.65
fraction (10 <sup>-2</sup> )	± 0.15	± 0.09	± 0.07	± 0.05	± 0.02	± 0.04	± 0.03	± 0.03

**TABLE 3. Physical properties of samples.**

particle size	humidity	temperature
Less than 74µm	Indoor humidity	36°

a 200-mesh steel screen. Then put samples into a 120-degree oven and dry for 12 hours to remove the moisture adsorbed during the grinding process. Table 3 shows the physical properties of samples.

Then, 39 samples of different proportion were weighed with a high-precision electronic scale, each sample is 200 mg and mixed evenly. The samples were pressed by a tablet press at a pressure of 24MPa for 4 minutes. Each pressed sheet is 13mm diameter disc-shaped sheets with smooth surfaces and no cracks. Finally, we used the vernier caliper to measure the thickness of the 39 coal-rock samples, and then calculated the absorption coefficient and the refractive index. Although the mass of each sample is the same, the thickness of the pressed sheet is not consistent because of the different densities of coal and rock. Table 4 shows the coal and rock pressures information.

Where the ratio of rock is the mass ratio of rock powder to the sample.

At the same time, we also prepared 33 Coal-HDPE samples and 33 rock- HDPE samples with different sparsity by using the procedure of preparing coal-rock samples. From pure HDPE to pure coal/rock, there are 33 samples with different sparsity degrees. Each Coal-HDPE or each Rock-HDPE sample has a mass of 100 mg and is pressed at 20 MPa for 3 minutes. Finally, 33 Coal-HDPE samples and 33 Rock-HDPE samples were prepared. The pressures information of the 66 samples is not listed here.

**C. DATA HANDLING**

Before collecting the time domain data, we turned on the TAS7500SP system for more than 30 minutes to keep the system stable. The signal obtained from terahertz light wave passing through the air as the background (reference signal), and the data obtained from terahertz light wave passing through the sample to be tested is used as the sample signal.

Each sample is measured three times at different positions, and the average value is taken as the time domain spectral signal of the sample. At this time, the time domain spectrum obtained is transformed into frequency domain spectrum by Fourier transform (FFT). And then the main optical parameters such as refractive index  $n(w)$ , extinction coefficient  $k(w)$  and absorption coefficient  $\alpha(w)$  are calculated by using the optical parameter extraction model proposed by Duvillaret *et al* [26], Dorney *et al* [27], and Vieweg *et al* [28]. The following is the formula for its calculation:

$$n(w) = \frac{\varphi(w)c}{wd} + 1 \tag{1}$$

$$k(w) = \frac{c}{wd} \ln \left\{ \frac{4n(w)}{\rho(w)[n(w) + 1]^2} \right\} \tag{2}$$

$$\alpha(w) = \frac{2wk(w)}{c} \tag{3}$$

where  $w$  is frequency,  $\varphi(w)$  is phase difference between sample signal and reference signal,  $\rho(w)$  is amplitude ratio of sample signal to reference signal,  $d$  and  $c$  is sample thickness(m) and speed of light respectively.

**III. RESULTS AND DISCUSSIONS**

**A. TERAHERTZ SPECTRAL CHARACTERISTICS OF COAL-ROCK**

We conducted THz experiments on 39 samples, of which 11 samples shown in Table 5 are selected for time-frequency domain analysis. After samples preparation, we use THz-TDs to obtain the time domain signal of coal-rock mixture samples which shown in Fig. 3(a). Compared with the background sample, the terahertz amplitude of these samples decreases caused by the surface reflection and absorption is decreasing with the decrease of rock ratio, and the attenuation phenomenon is becoming more and more obvious.

Frequency domain analysis is common in spectral analysis. Time-frequency conversion is usually used to transform the signal from time domain into frequency domain, and the correlation calculation is carried out to obtain the information beneficial to the research purpose. Fig. 3(b) is the spectrum diagram obtained by fast Fourier transform (FFT) in time domain spectrum. The bandwidth of air is about 4THz and that of coal-rock mixture sample is between 1.8~3THz. The bandwidth of each sample tends to shorten with the decrease

**TABLE 4. Thickness of coal and rock pressure sheets.**

Number	The ratio of rock /%	Thicknes s/mm	Number	The ratio of rock /%	Thickn ess/mm
1	0%	1.12	21	52%	0.96
(pure rock)					
2	5%	1.19	22	54%	0.92
3	10%	1.17	23	56%	0.88
4	15%	1.11	24	58%	0.91
5	20%	1.08	25	60%	0.90
6	22%	1.10	26	62%	0.86
7	24%	1.11	27	64%	0.89
8	26%	1.04	28	66%	0.98
9	28%	1.01	29	68%	0.89
10	30%	1.03	30	70%	0.90
11	32%	1.08	31	72%	0.84
12	34%	0.99	32	74%	0.89
13	36%	0.98	33	76%	0.93
14	38%	1.04	34	78%	0.93
15	40%	1.04	35	80%	0.92
16	42%	1.03	36	85%	0.98
17	44%	0.93	37	90%	0.85
18	46%	0.94	38	95%	0.86
19	48%	0.97	39	100%	0.86
(pure coal)					
20	50%	1.08			

**TABLE 5. Ratio of rock of 11-group coal-rock mixture samples.**

Numble	1	3	5	10	15	20
Ratio of rock	0%	10%	20%	30%	40%	50%
Numble	25	30	35	37	39	
Ratio of rock	60%	70%	80%	90%	100%	

of rock ratio. All samples have a peak amplitude at 0.5THz, and the peak amplitude gradually decreases with the decrease of rock ratio.

Fig. 3(c) and (d) shows that the absorption spectrum and the refractive index spectrum of coal-rock mixture samples with different ratio of rock calculated by the formula (1) and (3). It can be seen that, the absorption coefficients of each sample showed an upward trend in the frequency of 0.4-1.6 THz, while the refractive index of each sample maintains a steady curve in this frequency range. What's more, the absorption coefficients increased gradually on 0.4~1.6Hz with the decrease of rock, and the variation trend of refractive index of 11 samples is the same as of that of absorption coefficients with the decrease of rock shown in Fig. 3(d).

For observing the interaction between the different rock ratio of coal-rock mixtures samples and their response under terahertz light waves, the principal component analysis (PCA) was employed. PCA is a multivariate analysis method for converting a plurality of variables into a small number of linear non-related variables by orthogonal transform, and the converted set of variables is referred to as the principal components (PCs). PCs can reflect most of the information of the original variable and do not overlap each other, usually represented as a linear combination of the original variables. In addition, PCs fits the statistically significant variance and random measurement error in the data, which can propose the random error in the principal component as much as possible, so as to reduce the dimension of the complex data and minimize the influence of the measurement

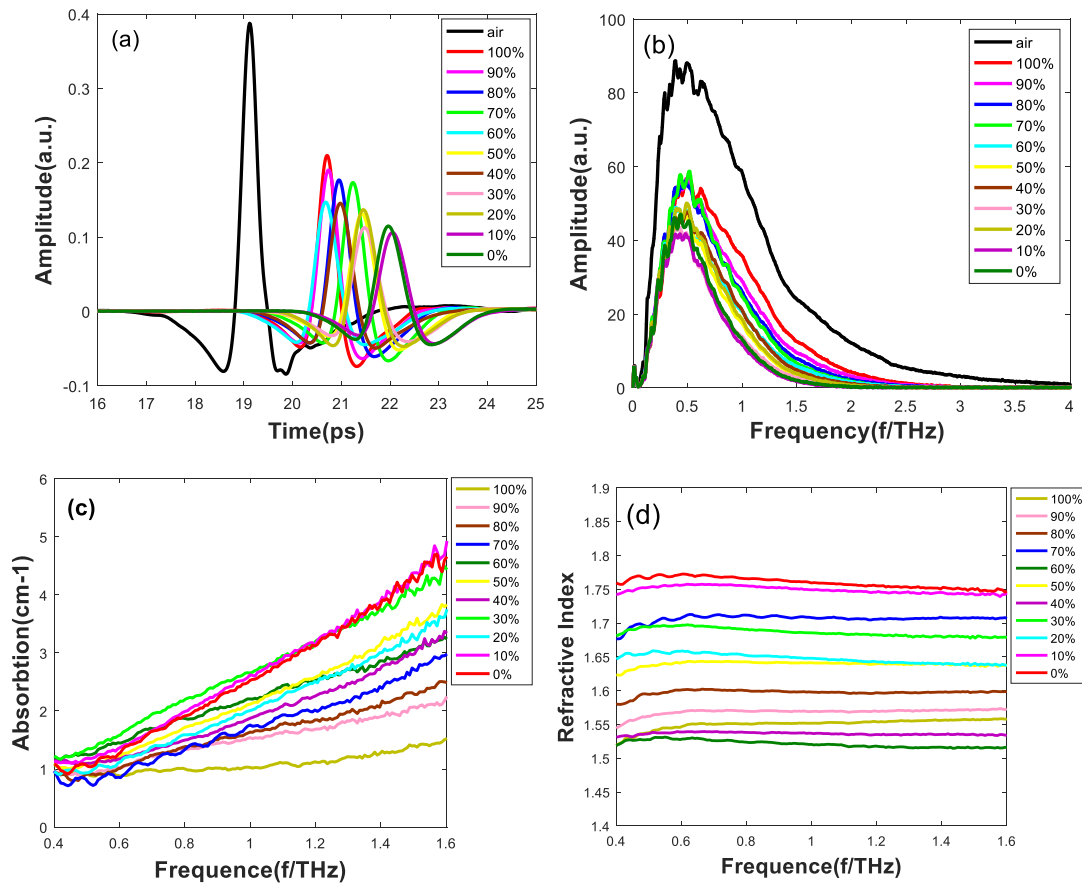


**FIGURE 3.** (a) Time domain spectrum, (b) Frequency domain spectrum, (c) Absorption coefficient spectrum, (d) Refractive spectrum of coal and rock mixtures samples with different ratio of rock.

error [29], [30]. Based on absorption spectra and refractive spectra in the 0.4~1.6THz frequency range, we used PCA algorithm to consider the absorption effect of different coal-rock mixtures samples.

First, the absorption coefficient and refractive index are taken as input respectively, PCs as the output. We analyzed the results of principal component calculation shown in Fig. 4(a), finding that the PC1 and PC2 describe 97.47% and 2.07% of information when taking absorption coefficient as input. When taking the refractive spectrum as input, the total contribution rate of PC1 and PC2 is 99.93%, with 99.55% of PC1, shown in Fig. 4(b). The results indicated that PCA has a good dimensionality reduction effect on the terahertz characteristic spectra of coal-rock samples. What's more, the PC1 extracted can represent almost all information of characteristic spectra of the coal-rock mixture samples, both the absorption spectrum and the refraction spectrum.

Second, in order to analyze the quantitative relationship between PCs and rock ratio of coal-rock samples, the PC1 was extracted because of its largest contribution rate. The scatter diagram of all samples' PC1 are shown in Fig. 4(c) and (d). In Fig. 4(c), with the rock ratio increasing, PC1 scores extracted by absorption spectrum decrease continuously, which is consistent with the regulation of absorption

coefficient reduction in Fig. 3(c). Finally, based on the downward trend of PC1, we built a linear model between PC1 scores and rock ratio of coal-rock samples, finding the correlation coefficient (R) of model is 0.8132. At the same time, we also established a linear model between refractive index and rock ratio, with a relatively small correlation of 0.6294, as shown in Fig. 4(d). The result that the PC1 score of absorption spectrum and refraction spectrum is basically distributed around the respective fitting lines represent obvious correlation between THz signal and rock ratio.

**B. QUANTITATIVE DETECTION MODEL OF COAL-ROCK MIXTURE SAMPLES**

In order to establish a corresponding quantitative model between the ratio of rock and THz signal, we tried to divide all the samples into two parts, of which 28 samples are training set for calculating a quantitative model, and the remaining 11 samples are prediction set for verifying the accuracy of the trained model. Back Propagation Neural Network (BPNN) is a kind of multi-layer feedforward neural network trained according to error reverse propagation algorithm [31]. It is the most widely used neural network at present [32]. Here, we first employed BPNN to build a model, the input of model is the absorption coefficient or refractive index of the sample in

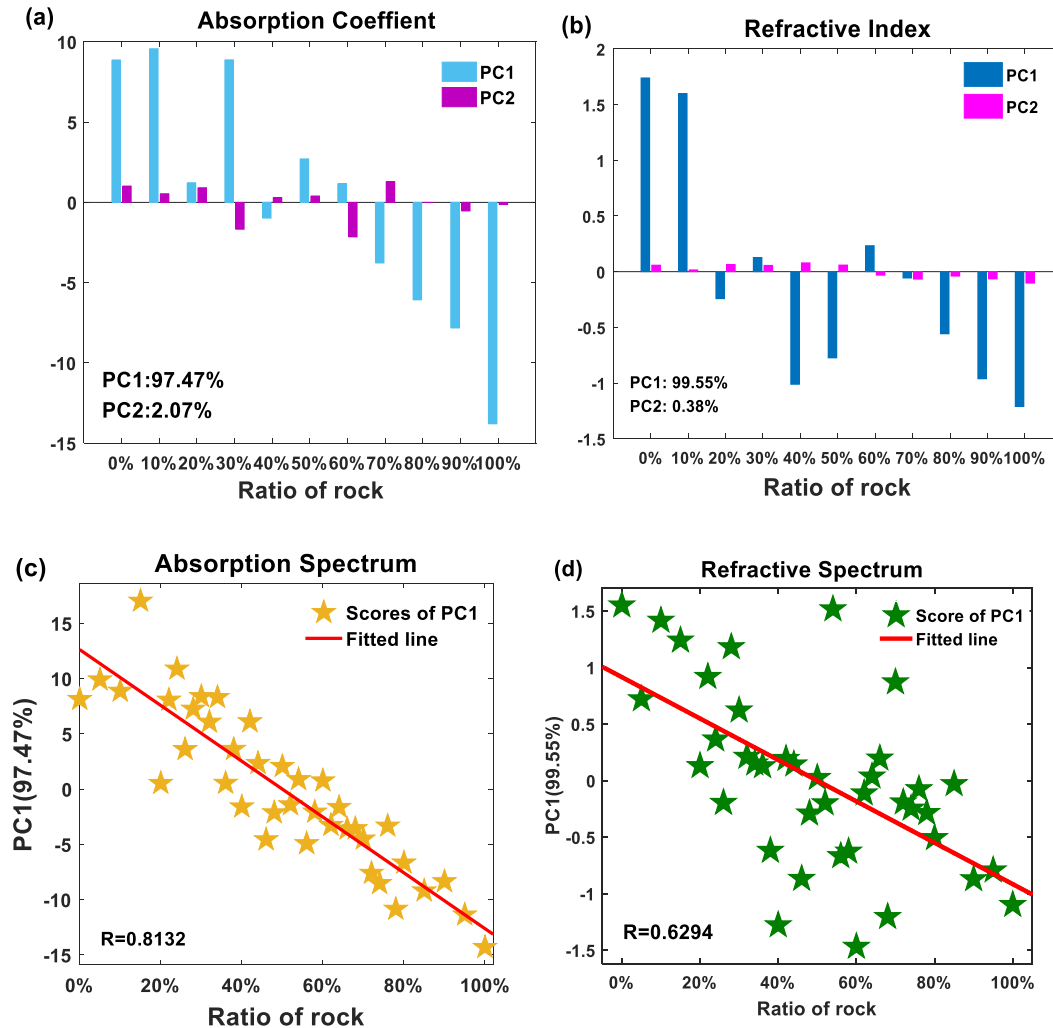


**FIGURE 4.** Principal component analysis (PCA) model built from different rock ratio of coal-rock mixture samples on the absorption spectrum and refractive spectrum within 0.4~1.6THz frequency. (a): PC1 and PC2 scores extracted from absorption spectrum of 11 different coal-rock mixture samples; (b): PC1 and PC2 scores extracted from refractive spectrum of 11 different coal-rock mixture samples; (c): PC1 score extracted from absorption spectrum of 39 coal-rock mixtures samples; (d): PC1 score extracted from refractive spectrum of 39 coal-rock mixtures samples.

a selected range of frequencies and the output of model is the predicted ratio of rock. In addition, we set up the intermediate layer of BPNN model as five layers.

We select 11 samples listed in table 5 as the prediction set of BPNN model because of their equal interval ratio and the left twenty-eight groups as the training set. Fig.5 (a) and (b) shows the predicted ratio of rock versus measured rock ratio of coal-rock samples with THz signal in Fig. 3(c) and (d) over the range from 0.4THz to 1.6THz as the input, respectively. The average detection time of BPNN model is 0.094 seconds. As expected, all the points are located near the reference (Ref.) line, which means the predicted value are close to the measured ratio of rock.

To evaluate the reliability and precision of the model, the correlation coefficient (R) and the root-mean square error (RMSE) are calculated. R represents the degree of linear correlation between the predicted value and the measured

value, and RMSE is the square root of the ratio of the square to the predicted number of the deviation between the predicted value and the measured value, which can measure the deviation between the predicted value and measured value. Hence, we used R and RMSE to evaluate the stability of established quantitative regression models. R and RMSE listed in Table 6 can better represent the correlation between detected ratio of rock and actual ratio of rock. As shown in Table 6, when the model takes the absorption coefficient of training set ranged from 0.4THz to 1.6THz as input, the R of training set exceed 97% and the prediction accuracy rate of this model exceed 90%. Table 6 also compares the model accuracy under different THz signal (absorption spectrum and refractive spectrum). When the model takes the refractive spectrum of training set ranged from 0.4THz to 1.6THz as input, the R of training set is 98.7% and the prediction accuracy rate of this model can reach 92.8%. The comparison indicated the

TABLE 6. Evaluation of model established by regression algorithm.

Method	Input parameter	Training Set (28)		Prediction set (11)	
		R	RMSE	R	RMSE
BPNN	Absorbance coefficient	97.1%	1.1%	90.4%	4.7%
	Refractive index	98.7%	0.7%	92.8%	3.8%
LSSVM	Absorbance coefficient	99.5%	0.4%	92.7%	4.1%
	Refractive index	99.6%	0.4%	95.7%	3.0%

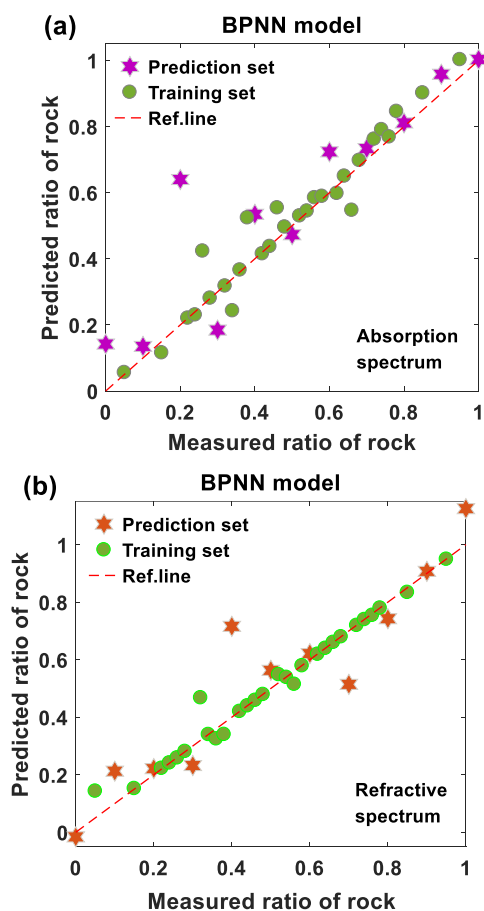


FIGURE 5. Prediction result of BPNN model based on (a) absorption spectrum, (b) refractive spectrum.

result of refractive spectrum ranged from 0.4THz to 1.6THz displays better performance than absorption spectrum ranged from 0.4THz to 1.6THz for the BPNN model.

Another regression algorithm, the least square support vector machine (LSSVM), was employed for comparing with the BPNN method [33]. LSSVM uses the least square linear

system as the loss function, instead of the traditional support vector machine using the quadratic programming problem. It can improve the accuracy of nonlinear signal processing [34]. In the process of LSSVM model building, the kernel function selects RBF\_kernel, the optimized parameter gam is 138, sig2 is 0.01. The training set and prediction set of LSSVM model are the same as those of BPNN. The average detection time of LSSVM model is 0.069 seconds. Fig. 6 show the predicted value of all samples with different input in LSSVM model. Comparing the Fig. 6(a) with (b), the predicted value of training set in (b) is closer to the Ref. line, which is the same as the information shown in Fig. 5. To analyze the accuracy of two coal-rock quantitative model, we listed the output result of rock ratio prediction in Table 6. As shown in Table 6, whatever the input is the absorption coefficient of training set or refractive index, the R of training set exceed 99% and the R of prediction set exceed 92% in LSSVM model. That means the LSSVM method performs better than BPNN method in coal-rock quantitative detection and the combination of THz spectroscopy and statistical methods can really improve the precision and could be used to detect quantitatively ratio of rock. The results together relative researches about quantitative analysis revealed that THz-TDs technology is expected to be effectively used for quantitative detection of coal and rock in coal mining face.

C. ANALYSIS ON THE SAMPLE SPARSITY

Ideally, the samples collected by sampling device in the mine are coal, rock, or a mixture of the two, so we discussed the problem of the rock powder ratio detection in the ideal state and proved feasibility of this method in section III. B. In practice, the samples collected by the sampling device have the presence of air, which has almost no influence on the above results because of little absorption of the dry air by terahertz waves. However, due to the addition of air, the actual sample states becomes coal-air, rock-air and coal-rock-air.



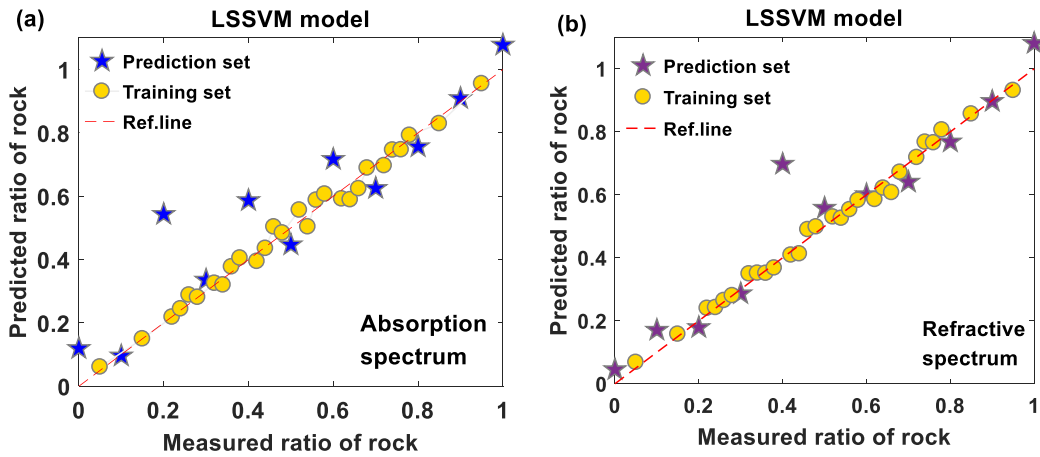


FIGURE 6. Prediction result of LSSVM model based on (a) absorption spectrum and (b) refractive spectrum.

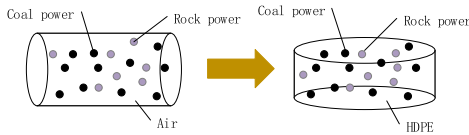


FIGURE 7. Equivalent coal-rock-air sample and equivalent coal-Rock-HDPE sample.

At this point, it is necessary to discuss the influence of sample sparsity on THz signal. The sparsity is the volume ratio of medium to sample. Therefore, two extremes of coal-rock sample, coal-air and rock-air, were analyzed.

Due to the complexity of the device experiment of gas-solid two-phase flow, the addition of polyethylene was used to simulate a certain static state of gas-solid two-phase flow. Meanwhile, the sparsity of samples could be changed by changing the contents of polyethylene so as to achieve the purpose of this study. The key to online characterization of coal and rock is to replace the sample of gas-solid two-phase flow state with pressure sheet, as shown in Fig.7.

Lambert Beer’s law describes the direct relationship between the absorption of substance to light, the thickness of the absorbing medium and the concentration of the absorbing material [35]:

$$A = \epsilon dc \tag{4}$$

where,  $A$  is the absorbance,  $\epsilon$  is the absorption coefficient.  $d$  is the sample thickness, and  $c$  is the speed of light. According to formula (4), when the thickness is consistent, the absorbance of specific sample is only positively correlated with the sample concentration. Therefore, we assume that the absorption coefficients of coal and rock are  $a$  and  $b$ , respectively. Since the absorption of HDPE to terahertz wave is almost zero, the absorbance of the mixture of Coal-Rock-HDPE is  $A$ . For all sampling points:

$$\begin{cases} a_1x_1 + b_1x_2 = A_1 \\ a_2x_1 + b_2x_2 = A_2 \end{cases} \tag{5}$$

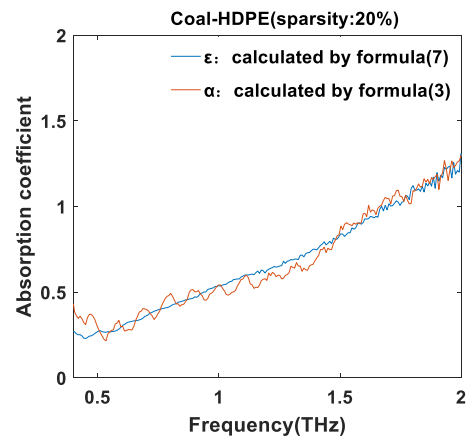


FIGURE 8. THz absorption coefficient of Coal-HDPE sample.

The equation (5) is expressed in matrix form, and it can be obtained as follows:

$$\begin{bmatrix} a_1 & b_1 \\ a_2 & b_2 \end{bmatrix} \cdot \begin{bmatrix} x_1 \\ x_2 \end{bmatrix} = \begin{bmatrix} A_1 \\ A_2 \end{bmatrix} \tag{6}$$

The simplification formula (6) can be obtained:

$$MX = A \tag{7}$$

Through formula (7), we can also calculate the amount of each component in a sample.

The  $\epsilon$  calculated by Formula (7) is only the absorption coefficient of pulverized coal to THz wave, while the  $\alpha$  calculated by formula (3) is the absorption coefficient and scattering of pulverized coal to THz wave. Taking Coal-HDPE as examples. We compare  $\epsilon$  with  $\alpha$  shown in Fig.8. Obviously,  $\alpha$  has obvious fluctuation, which may be caused by the scattering of THz wave by pulverized coal. However,  $\alpha$  and  $\epsilon$  rise by the same amount in the range of 0.4~2THz, and almost at the same level. Therefore, in this experiment, we can ignore the THz scattering of the sample.

The presence of air in the sample inevitably affect the sample sparsity, which may affect the accuracy of coal-rock

interface characterization. Therefore, we study the effect of sparsity on THz signal. Firstly, 33 samples with different mass ratios of coal-HDPE and 33 samples with different mass ratios of rock-HDPE were converted into different volume ratios, namely sparsity. Coal-HDPE and Rock-HDPE are taken as research objects respectively. The terahertz signal of pure HDPE was taken as the reference signal, and the remaining 32 terahertz signal of Coal-HDPE or Rock-HDPE samples with different sparsity was taken as the sample signal. We obtain time domain signal of Coal-HDPE and Rock-HDPE, respectively. Fig.9 shows time-domain spectrum of Coal-HDPE and Rock-HDPE. We expected to extract and fuse multiple features from the time-domain and frequency-domain to analyze the sensitivity of different sparsity to THz signals. Second, the time delay and peak values in the time domain are extracted as two THz features. The signal in the time domain cannot represent all information of samples, so we converted the time domain into frequency domain by fast Fourier transform. We also extracted the absorption coefficients and refractive index of samples at 1THz frequency, calculated by formula (2) and formula (3). The selection of 1THz mainly because the signal of the sample on 1THz is more stable and has a smaller slope than that near the peak. Finally, we standardized these four characteristics to remove the unit limitation of the data.

According to different sparsity boundaries, 32 samples of Coal-HDPE were divided into two categories, such as sparsity below 10% and over 10%, sparsity below 20% and over 20%, sparsity below 30% and over 30%, sparsity below 40% and over 40%, etc. And 32 Rock-HDPE samples were classified in the same way. The detail of classification is shown in Table 7. Support Vector Machine (SVM) is a classification algorithm established on the basis of statistics. The method is suitable for solving the problem of small sample and nonlinear pattern classification based on the principle of structural risk minimization. In the experiment, the kernel function of support vector machine is the radial basis function. In addition, the network optimization method is used to optimize two parameters, penalty factor  $c$  and kernel function  $g$ .

We took the four normalized characteristics in the terahertz time-frequency domain as input parameters for modeling. Due to the limited number of samples, 32 samples were divided into 24 calibration sets and 8 prediction sets for each modeling. For Coal-HDPE and Rock-HDPE, 9 classification modeling was performed respectively. The results are shown in Table 7. The classification accuracy are represented by  $R$ .

In Table 7, we found that SVM can classify and predict the sparsity of Coal-HDPE and Rock-HDPE regardless of the sparsity boundary, and the prediction accuracy is more than 87.5%. When the sparsity of the Coal-HDPE sample is higher than 20%, the accuracy of SVM for the classification of the sparsity reaches 100%. When the sample sparsity of Rock-HDPE is higher than 10%, the classification accuracy of the sparsity reaches 100%. Thus it can be seen that, SVM can realize the classification of sample sparsity.

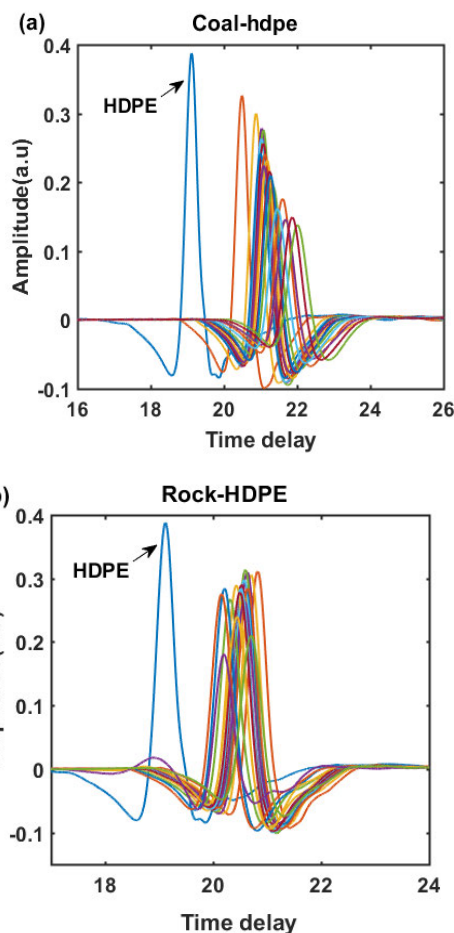


FIGURE 9. (a) Time-domain spectrum of Coal-HDPE with different sparsity, (b) Time-domain spectrum of Rock-HDPE with different sparsity.

Combining the classification accuracy of Coal-HDPE and Rock-HDPE, we found that the classification accuracy is higher when the sample sparsity is higher than 20%. That is to say, when the sparsity of the sample is higher than 20%, the results of detecting coal and rock by THz-TDs are more reliable. Sparsity analysis provides the basis for the design of the coal mining machine sampling equipment in the coal face in the future.

#### D. COAL-ROCK INTERFACE CHARACTERIZATION

After the coal-rock proportion is quantified and the sample sparsity is discussed, we need to go back to ultimate goal that characterization of coal-rock interface. Fig. 10 shows the cutting state of the shearer drum embedded in the rock. We expected to estimate the height of the shearer drum embedded in the rock by the ratio of the rock occupying the total sample. Theoretically, when the drum is embedded in the rock layer, the ratio of rock powder generated by cutting in one circle to all the dust is the ratio of rock volume cut to total volume cut, including coal seam and rock layer. Since the thickness of the coal seam cut by the drum is the same as that of rock stratum, we use the surface area ratio within one circle instead of the volume ratio. The geometric relation is

TABLE 7. The result of classification accuracy.

Classification boundary of sparsity	Coal-HDPE		Rock-HDPE	
	Calibration set	Prediction set	Calibration set	Prediction set
10%	100%(24/24)	100%(8/8)	100%(24/24)	87.5%(7/8)
20%	100%(24/24)	87.5%(7/8)	100%(24/24)	100%(8/8)
30%	100%(24/24)	100%(8/8)	100%(24/24)	100%(8/8)
40%	100%(24/24)	100%(8/8)	100%(24/24)	100%(8/8)
50%	100%(24/24)	100%(8/8)	100%(24/24)	100%(8/8)
60%	100%(24/24)	100%(8/8)	100%(24/24)	100%(8/8)
70%	100%(24/24)	100%(8/8)	100%(24/24)	100%(8/8)
80%	100%(24/24)	100%(8/8)	100%(24/24)	100%(8/8)
90%	100%(24/24)	100%(8/8)	100%(24/24)	100%(8/8)

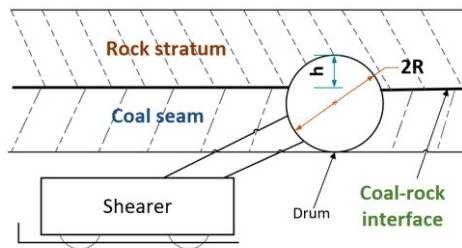


FIGURE 10. Coal-rock interface detection.

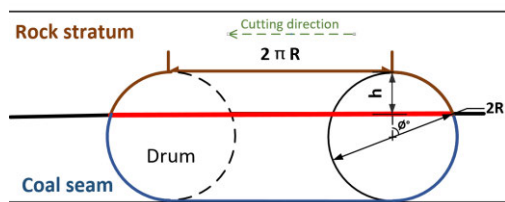


FIGURE 11. Cutting mode of drum cutting for one cycle.

expressed as:

$$P = \frac{S_r \rho_r}{S_r \rho_r + S_c \rho_c} \tag{8}$$

P is rock volume accounts for the total volume of coal and rock,  $S_r$  is the surface area of rock layer cut,  $S_c$  is the surface area of coal layer cut.  $\rho_c, \rho_r$  are the density of coal and rock respectively.

Fig. 11 shows the drum cutting mode of shearer, where h is the height of the shearer drum embedded in the rock, which can be estimated by  $S_r$ :

$$\cos \theta = \frac{R - h}{R} \tag{9}$$

$$S_r = 2\pi R h + \frac{\theta \pi R^2}{180} - R(R-h) \sin \theta \tag{10}$$

$$S_c = S - S_r \tag{11}$$

$R, \theta$  are the radius of the drum and angle shown in Fig. 9. S is the surface area of a cylinder cut. Ideally, when there is no coal seam caving except the cutting part, S is a fixed value:

$$S = 5\pi R^2 \tag{12}$$

By using formula (8)-(12), the coal-rock interface model can be established to estimate h. In this way, our ultimate goal, on-line coal-rock interface characterization, is achieved by using THz-TDs.

#### IV. CONCLUSION

The intelligent mining face require the automatic height adjustment of the shearer to realize. Such automation is required to complete by automatic coal and rock detection technology. This research has demonstrated how THz-TDs can be utilized to detect the ratio of rock around the shearer, and how the ratio of rock can be used to perform online characterization of the coal-rock interface.

During the establishment of the coal and rock quantitative detection model, both BPNN and LSSVM models based on refractive index data can accurately quantitatively detect coal and rock samples. Compared with the BPNN model, LSSVM performs better in predicting rock ratio regardless of which THz signal is used as parameter. Obviously, the LSSVM model based on refraction spectrum as input can meet the prediction accuracy requirements. The quantitative detection model is combined with the theoretical model built in section III. D to prove the possibility of coal-rock interface characterization. What's more, in terms of sample sparsity analysis, we found that the SVM can accurately classify sparsity, and the classification accuracy is higher when sparsity is higher than 20%.

All the obtained results implied that the novel method of on-line coal-rock interface characterization using THz-TDs could not only detect coal-rock interface online, but also adjust the height of the next cut of shearer in time. Therefore, the proposed method can accelerate the development process

of intelligent mines, and it is of great significance to ensure the safety of underground mining person, prolong the life of shearer and improves the production efficiency.

## ACKNOWLEDGMENT

(Jing Yu and Xin Wang contributed equally to this work.)

## REFERENCES

- [1] K.-D. Gao, W.-B. Xu, S.-B. Jiang, and C.-L. Du, "Factors affecting thin coal seam shearer drum coal-loading performance by a model test method," *J. Central South Univ.*, vol. 26, no. 6, pp. 1619–1636, Jun. 2019.
- [2] M. Kingshott and M. Graham, "Coal age—A Longwall look at tomorrow," in *Proc. Coal Operators' Conf.*, 1998, pp. 343–351.
- [3] N. Innaurato, C. Oggeri, P. P. Oreste, and R. Vinai, "Experimental and numerical studies on rock breaking with TBM tools under high stress confinement," *Rock Mech. Rock Eng.*, vol. 40, no. 5, pp. 429–451, Oct. 2007.
- [4] O. Su and N. Ali Akcin, "Numerical simulation of rock cutting using the discrete element method," *Int. J. Rock Mech. Mining Sci.*, vol. 48, no. 3, pp. 434–442, Apr. 2011.
- [5] S. Dewangan, S. Chattopadhyaya, and S. Hloch, "Wear assessment of conical pick used in coal cutting operation," *Rock Mech. Rock Eng.*, vol. 48, no. 5, pp. 2129–2139, Sep. 2015.
- [6] Y. Wang, C. Liu, and Y. Liao, "Electromechanical dynamic analysis for the DTC induction motor driving system of the unmanned longwall shearer drum," *Cluster Comput.*, vol. 22, no. S6, pp. 13325–13336, Nov. 2019.
- [7] S. Hao, S. Wang, R. Malekian, B. Zhang, W. Liu, and Z. Li, "A geometry surveying model and instrument of a scraper conveyor in unmanned longwall mining faces," *IEEE Access*, vol. 5, pp. 4095–4103, 2017.
- [8] X. Wang, K.-X. Hu, L. Zhang, X. Yu, and E.-J. Ding, "Characterization and classification of coals and rocks using terahertz time-domain spectroscopy," *J. Infr., Millim., THz Waves*, vol. 38, no. 2, pp. 248–260, Feb. 2017.
- [9] H. Wang and Q. Zhang, "Dynamic identification of coal-rock interface based on adaptive weight optimization and multi-sensor information fusion," *Inf. Fusion*, vol. 51, pp. 114–128, Nov. 2019.
- [10] H. Wang, M. Huang, S. Lu, Z. Qi, J. Du, J. Yuan, Z. Wu, M. Wang, X. Pang, G. Cen, and C. Liang, "A dynamic coal-rock interface recognition model based on cutting acoustic emission and fuzzy D-S theory," in *Proc. IEEE 4th Inf. Technol., Netw., Electron. Autom. Control Conf. (ITNEC)*, Jun. 2020, pp. 274–279.
- [11] G. Zhang, Z. Wang, L. Zhao, Y. Qi, and J. Wang, "Coal-rock recognition in top coal caving using bimodal deep learning and Hilbert-huang transform," *Shock Vibrat.*, vol. 2017, pp. 1–13, Jan. 2017.
- [12] Z. Wang, G. Zhang, and L. Zhao, "Recognition of rock-coal interface in top coal caving through tail beam vibrations by using stacked sparse autoencoders," *J. Vibroeng.*, vol. 18, no. 7, pp. 4261–4275, Nov. 2016.
- [13] L. Si, Z.-B. Wang, and G. Jiang, "Fusion recognition of shearer coal-rock cutting state based on improved RBF neural network and D-S evidence theory," *IEEE Access*, vol. 7, pp. 122106–122121, 2019.
- [14] L. Si, Z. Wang, Y. Liu, and C. Tan, "Online identification of shearer cutting state using infrared thermal images of cutting unit," *Appl. Sci.*, vol. 8, no. 10, p. 1772, Sep. 2018.
- [15] P. Jepsen, D. Cooke, and M. Koch, "Terahertz spectroscopy and imaging—modern techniques and applications," *Laser Photon. Rev.*, vol. 6, no. 3, p. 418, 2012.
- [16] P. Salén, M. Basini, S. Bonetti, J. Hebling, M. Krasilnikov, A. Y. Nikitin, G. Shamuilov, Z. Tibai, V. Zhaunerchyk, and V. Goryashko, "Matter manipulation with extreme terahertz light: Progress in the enabling THz technology," *Phys. Rep.*, vols. 836–837, pp. 1–74, Dec. 2019.
- [17] Y. Jiang, H. Ge, and Y. Zhang, "Quantitative analysis of wheat maltose by combined terahertz spectroscopy and imaging based on boosting ensemble learning," *Food Chem.*, vol. 307, Mar. 2020, Art. no. 125533.
- [18] S. Sommer, T. Raidt, B. M. Fischer, F. Katzenberg, J. C. Tiller, and M. Koch, "THz-spectroscopy on high density polyethylene with different crystallinity," *J. Infr., Millim., THz Waves*, vol. 37, no. 2, pp. 189–197, Feb. 2016.
- [19] L. Liang, S. Tang, M. Tong, and H. Dong, "Study on the detection method of the granularity of pulverized coal based on THz time-domain chaos features," *Spectrosc. Spectral Anal.*, vol. 39, no. 5, pp. 1392–1397, 2018.
- [20] H. Zhao, L. Zhang, S. Huang, and C. Zhang, "Terahertz wave generation from noble gas plasmas induced by a wavelength-tunable femtosecond laser," *IEEE Trans. THz Sci. Technol.*, vol. 8, no. 3, pp. 299–304, May 2018.
- [21] H. Zhan, S. Wu, R. Bao, L. Ge, and K. Zhao, "Qualitative identification of crude oils from different oil fields using terahertz time-domain spectroscopy," *Fuel*, vol. 143, pp. 189–193, Mar. 2015.
- [22] H. Zhan, N. Li, K. Zhao, Z. Zhang, C. Zhang, and R. Bao, "Terahertz assessment of the atmospheric pollution during the first-ever red alert period in Beijing," *Sci. China Phys., Mech. Astron.*, vol. 60, no. 4, Apr. 2017, Art. no. 044221.
- [23] H. Zhan, K. Zhao, R. Bao, and L. Xiao, "Monitoring PM2.5 in the atmosphere by using terahertz time-domain spectroscopy," *J. Infr., Millim., THz Waves*, vol. 37, no. 9, pp. 929–938, Sep. 2016.
- [24] S. Yan, D. Wei, M. Tang, C. Shi, M. Zhang, Z. Yang, C. Du, and H. Cui, "Determination of critical micelle concentrations of surfactants by terahertz time-domain spectroscopy," *IEEE Trans. THz Sci. Technol.*, vol. 6, no. 4, pp. 532–540, Jun. 2016.
- [25] X. Zhang and J. Xu, *Introduction to THz Wave Photonics*. New York, NY, USA: Springer, 2010.
- [26] L. Duvillearet, F. Garet, and J.-L. Coutaz, "Highly precise determination of optical constants and sample thickness in terahertz time-domain spectroscopy," *Appl. Opt.*, vol. 38, no. 2, pp. 409–415, Oct. 1999.
- [27] D. M. Mittleman, R. G. Baraniuk, and T. D. Dorney, "Material parameter estimation with terahertz time-domain spectroscopy," *J. Opt. Soc. Amer. A, Opt. Image Sci.*, vol. 18, no. 7, pp. 1562–1571, Jul. 1996.
- [28] N. Vieweg, F. Rettich, A. Deninger, H. Roehle, and M. Schell, "Terahertz-time domain spectrometer with 90 dB peak dynamic range. Journal of Infrared," *Millim. THz Waves*, vol. 35, no. 10, pp. 823–832, 2014.
- [29] S. W. X. Tu Zhang Xiong and T. Chen, "Principal component analysis for transgenic cotton seeds based on terahertz time domain spectroscopy system," *Acta Photonica Sinica*, vol. 44, no. 4, pp. 176–181, 2015.
- [30] S. Mishra, U. Sarkar, S. Taraphder, S. Datta, D. Swain, R. Saikhom, S. Panda, and M. Laishram, "Multivariate statistical data analysis-principal component analysis (PCA)," *Int. J. Livestock Res.*, vol. 7, no. 5, pp. 60–78, 2017.
- [31] H. Hua, X. Xie, J. Sun, G. Qin, C. Tang, Z. Zhang, Z. Ding, and W. Yue, "Graphene foam chemical sensor system based on principal component analysis and backpropagation neural network," *Adv. Condens. Matter Phys.*, vol. 2018, pp. 1–8, Jan. 2018.
- [32] F. Yu and X. Xu, "A short-term load forecasting model of natural gas based on optimized genetic algorithm and improved BP neural network," *Appl. Energy*, vol. 134, pp. 102–113, Dec. 2014.
- [33] R. M. Adnan, Z. Liang, S. Heddham, M. Zounemat-Kermani, O. Kisi, and B. Li, "Least square support vector machine and multivariate adaptive regression splines for streamflow prediction in mountainous basin using hydro-meteorological data as inputs," *J. Hydrol.*, vol. 586, Jul. 2020, Art. no. 124371.
- [34] F. Kaytez, M. C. Taplamacioglu, E. Cam, and F. Hardalac, "Forecasting electricity consumption: A comparison of regression analysis, neural networks and least squares support vector machines," *Int. J. Electr. Power Energy Syst.*, vol. 67, pp. 431–438, May 2015.
- [35] X. Song and L. Liu, "A regression model of color value and substance concentration of colored solution based on lambert beer's law," in *Proc. Int. Conf. Cyber Secur. Intell. Anal.*, vol. 1146, Feb. 2020, pp. 814–820.



**JING YU** was born in 1996. She received the B.S. degree in information engineering from Fuyang Normal University, Fuyang, China, in 2018. She is currently pursuing the master's degree with the China University of Mining and Technology, Xuzhou, Jiangsu, China. Her research interests include nondestructive testing of THz wave and THz spectroscopy.



**XIN WANG** was born in 1982. He received the Ph.D. degree in information and communication engineering from the China University of Mining and Technology, Xuzhou, China, in 2017. He currently works as a Researcher with the Internet of Things Center, China University of Mining and Technology, and a Teacher at the Jiangsu Vocational Institute of Architectural Technology, Xuzhou. His research interests include nondestructive testing of THz wave and THz spectroscopy.



**JIANGBO JING** was born in 1993. He received the B.S. degree in communication engineering from the Hebei University of Science and Technology, in 2017. He is currently pursuing the M.S. degree with the China University of Mining and Technology, Xuzhou, Jiangsu, China. His research interest includes the semantic description of mines.

...



**ENJIE DING** was born in 1962. He received the Ph.D. degree in control theory and control engineering from the China University of Mining and Technology, Xuzhou, China, in 1999. He currently works as a Professor, a Doctoral Supervisor, and an Academic Backbone at the China University of Mining and Technology. His research interests include mine integrated automation and the mine Internet of Things.